Protein Adsorption and Coordination-Based End-Tethering of Functional Polymers on Metal–Phenolic Network Films

*Blaise L. Tardy,[†] Joseph J. Richardson, Vichida Nithipipat, Kristian Kempe,[‡] Junling Guo, Kwun Lun Cho, Md. Arifur Rahim, Hirotaka Ejima,[§] and Frank Caruso**

ARC Centre of Excellence in Convergent Bio-Nano Science and Technology, and the Department of Chemical Engineering, The University of Melbourne, Parkville, Victoria 3010, Australia

Keywords: MPN, Protein Fouling, Stealth, Layer-by-Layer, Mussel-Inspired Chemistry

ABSTRACT

Metal–phenolic network (MPN) coatings have generated increasing interest owing to their biologically inspired nature, facile fabrication, and near-universal adherence, especially for biomedical applications. However, a key issue in biomedicine is protein fouling, and the adsorption of proteins on tannic acid-based MPNs remains to be comprehensively studied. Herein, we investigate the interaction of specific biomedically relevant proteins in solution

(bovine serum albumin (BSA), immunoglobulin G (IgG), fibrinogen) and complex biological media (serum) using layer-by-layer-assembled tannic acid/Fe^{III} MPN films. When Fe^{III} was the outermost layer, galloyl-modified poly(2-ethyl-2-oxazoline) (P(EtOx)-Gal) could be grafted to the films through coordination bonds. Protein fouling and bacterial adhesion were greatly suppressed after functionalization with P(EtOx)-Gal and the mass of adsorbed protein was reduced by 44–92%. Interestingly, larger proteins adsorbed more on both the MPNs and P(EtOx)-functionalized MPNs. This study provides fundamental information on the interactions of MPNs with single proteins, mixtures of proteins as encountered in serum, and the noncovalent, coordination-based, functionalization of MPN films.

INTRODUCTION

Methods for depositing thin films are of immense scientific and technological interest, as they dominate the interaction between the coated material and the surrounding environment.[1] Versatile film formation strategies have recently been developed by exploiting the material-independent adherent capabilities of phenolic compounds.[2-4,5] For example, we recently reported the assembly of metal–phenolic network (MPN) films prepared from natural phenolic building blocks (e.g., tannins, tannic acid (TA), gallic acid) via the coordination cross-linking of metal ions (e.g., Fe^{III}, Cu^{II}).[5-7] Additionally, synthetic derivatives, such as multi-arm polyethylene glycol (PEG) polymers functionalized with catechol end groups, have been assembled by coordination into capsules that showed reduced fouling depending on the PEG content.[8,9] However, TA and Fe^{III} are both known to interact with proteins, where tannins are traditionally quantified by precipitation assays with proteins in food and leather, and induce cell coagulation,[10,11] whereas iron oxide particles display strong interactions with proteins when

studied in culture media.[12,13] Nevertheless, the fouling properties of MPN films and methods for reducing the fouling properties of TA-based MPN films have not been extensively studied. For example, a promising technique used for other metal–organic materials is chelation-based end-tethering,[14] which could offer a route, currently unexplored, for post-modifying MPN films with low-fouling polymers. Fundamental studies on protein adsorption onto MPN films and the functionalization of MPN films for reduced fouling would provide useful insights for a wide scope of biomedical applications.

Herein, we quantitatively investigate the adsorption of proteins, i.e., bovine serum albumin (BSA), immunoglobulin G (IgG), and fibrinogen, and complex biological media, namely fetal bovine serum (FBS), on MPN films using a quartz crystal microbalance (QCM) (**Figure 1**). The MPN films were prepared by the layer-by-layer (LbL) assembly method (**Figure 1a–d**).[15,16] LbL assembly[1,17] offers the possibility of studying the effect of the outermost (last adsorbed) layer on the surface properties of the resulting films,[15,18] for example, to distinguish which building block (TA or Fe^{III}) plays a more important role in governing MPN–protein interactions (**Figure 1e**). This enables a better understanding of to the biological interactions of MPNs and tannic acid-based materials.[19,20] In contrast to previous studies on the covalent modification of polyphenol films,[21,22] herein we demonstrate the use of coordination-based end-tethering with galloyl-terminated poly(2-ethyl-2-oxazoline) (P(EtOx)-Gal) in significantly reducing the amount of adsorbed proteins on the MPN films (**Figure 1f–h**). The noncovalent nature of the galloyl–metal interaction allows for the facile and tunable functionalization of MPN coatings. This functionalization method, along with the properties imparted by the P(EtOx) provides new opportunities for the fabrication of MPN films with reduced biofouling.

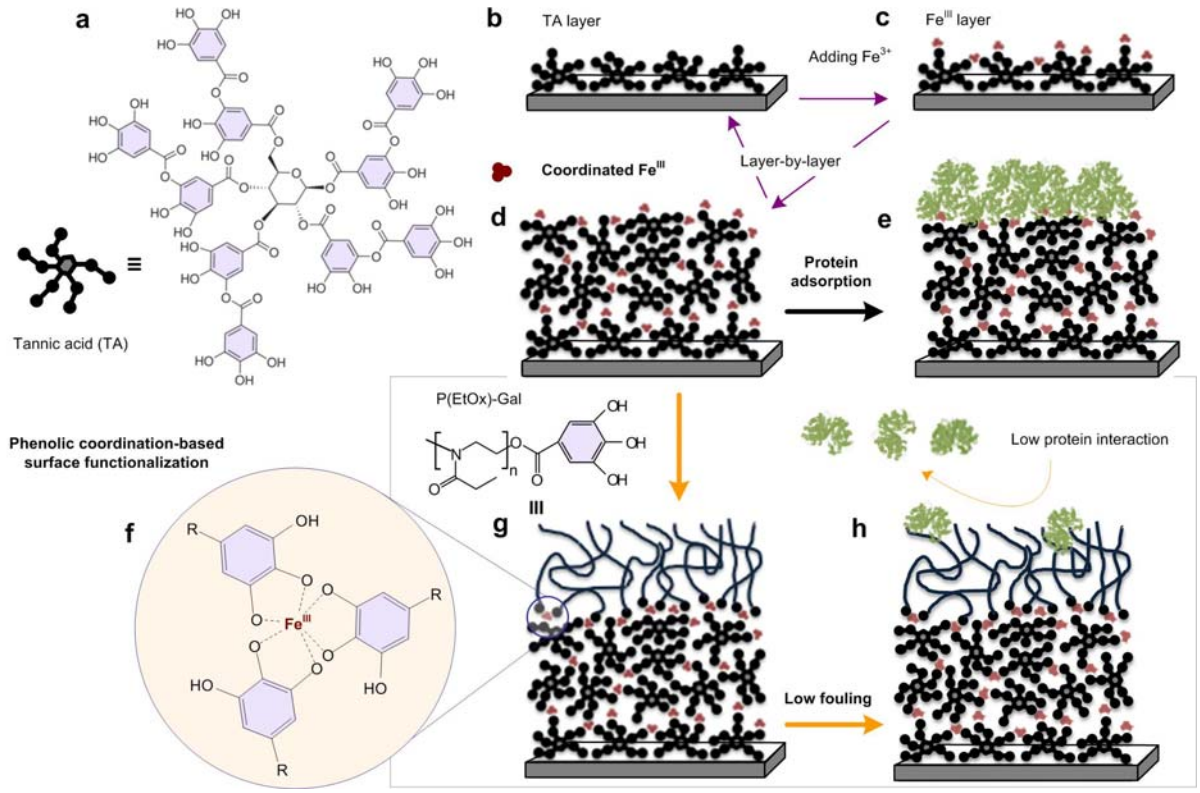

Figure 1. Illustration of the TA/Fe^{III} LbL assembly process and subsequent fouling on nonfunctionalized (pristine) and P(EtOx)-Gal-functionalized films. (a) Molecular structure of tannic acid (TA). (b–d) LbL assembly of TA/Fe layers on a planar substrate, whereby the composition of the last layer can be TA or Fe^{III}. (e) Affinity of proteins with LbL-assembled MPNs. Films capped with either Fe^{III} or TA both showed large mass increases when incubated with proteins. (f) Molecular structure of coordination between the galloyl groups of TA and/or P(EtOx)-Gal with Fe^{III}. (g) Phenolic coordination-based surface functionalization of LbL-assembled MPNs with P(EtOx)-Gal to reduce protein fouling (h).

MATERIALS AND METHODS

Materials. High-purity water with a resistivity of 18.2 MΩ cm was obtained from an in-line Millipore RiOs/Origin water purification system. The pH of solutions was measured with a

Mettler-Toledo MP220 pH meter. Unless otherwise noted, all chemicals were used as received. FBS was obtained from Gibco. 2-Ethyl-2-oxazoline and methyl tosylate were purchased from Sigma-Aldrich, distilled to dryness, and stored under argon. Acetonitrile, phosphate-buffered saline (PBS) tablets, TA, iron(III) chloride hexahydrate ($FeCl_3 \cdot 6H_2O$), IgG from bovine serum, BSA and fibrinogen of bovine source, poly(ethylene imine) (PEI), and quartz slides were purchased from Sigma-Aldrich. QCM crystals (9 MHz) were purchased from Kyushu Dentsu Co., Ltd., Japan. For the quartz crystal microbalance with dissipation monitoring (QCM-D) measurements, the crystals were purchased from Q-Sense, Sweden. The LIVE/DEAD BacLight Bacterial Viability Kit L7012 was purchased from Molecular Probes Inc.

Substrate Preparation. Before layer formation, gold-coated QCM crystals or quartz slides were cleaned by exposure to Piranha solution (70:30 v/v 97% sulfuric acid/30% hydrogen peroxide), followed by washing with water and ethanol, and drying with nitrogen gas. *Caution! Piranha solution is highly corrosive. Extreme care should be taken when handling piranha solution and only small quantities should be prepared.*

MPN Film Formation. Layer deposition and subsequent polymer or protein adsorption were monitored using QCM and QCM-D. The film was prepared as previously described.[15] From stock solutions of 40 mg mL^{-1} TA (stored at 4 °C for a maximum of 7 days), 0.4 mg mL^{-1} solutions of TA were prepared in water. QCM crystals or multi-well plates (for bacterial adsorption assays) were exposed to this solution for 10 min. Thereafter, the surface was washed with water. For the next layer deposition, the substrate was exposed to an aqueous solution of 0.1 mg mL^{-1} of $FeCl_3 \cdot 6H_2O$ for 10 min and subsequently rinsed with water. This process was repeated for the desired number of times (**Figure 1b–d**). After MPN deposition, the coated

substrate was exposed to a polymer (1 mg mL^{-1}) and/or protein solution without pH adjustment, unless otherwise specified.

QCM Measurements. Quantitative measurements of protein and polymer adsorption were performed using QCM. Specifically, for the mass adsorption studies in air, a QCM device (Hewlett−Packard) equipped with ∼9 MHz electrodes (resonance frequency) was used. After each adsorption step, the crystal was placed in the frequency counter and the resonance frequency of the crystal was recorded. The adsorbed mass, which corresponds to a decrease in resonance frequency (Δf), was determined using the formula:

$$\text{Mass density (g m}^{-2}) = -\Delta f\,(\text{Hz}) \times 2.73 \times 10^{-5}$$

QCM-D was performed using a Q-sense E4 (Q-sense, Sweden) instrument to monitor the adsorption in real time. Changes in the resonance frequency (Δf) and dissipation (ΔD) were recorded at 23 °C. Normalized frequencies using the third overtone were measured. An adsorption time of 10 min and washing time of 10 min were used.

Atomic Force Microscopy (AFM) Measurement of Root Mean Squared Roughness (R_{RMS}). AFM images were captured on an MFP-3D Asylum Research instrument. Typical scans were recorded in alternating current mode with ultra-sharp SiN gold-coated cantilevers (NT-MDT). Films were formed on quartz slides with a PEI (1 mg mL^{-1} in 500 mM NaCl solution) primer layer.[15] R_{RMS} values were calculated from 5 × 5 μm^2 scanned areas on the substrates.

Contact Angle Measurements. Static and advancing water contact angles of the coated quartz substrates were measured using a Model 200 standard goniometer (Ramé-Hart, USA). All contact angles were measured using a 10 μL water droplet at ambient temperature. Films were formed on quartz slides with a PEI (1 mg mL^{-1} in 500 mM NaCl solution) primer layer.

X-Ray Photoelectron Spectrometry (XPS) Measurements. XPS spectra were recorded on a VG ESCALAB 220i-XL spectrometer equipped with a monochromic Al Kα X-ray source with an emitted photon energy of 1486.6 eV at 10 kV and 12 mA. Measurements were processed at a step size of either 0.5 eV (wide scans) or 0.5 eV (region scans). Film samples (on QCM gold chips) were screwed to Al holders, and samples were examined in the analysis chamber at a typical operating pressure of $\sim 1 \times 10^{-9}$ Pa.

UV-Visible (UV-Vis) Spectroscopy Measurements. UV-Vis spectroscopy measurements were performed on a Varian Cary 4000 UV-vis spectrophotometer. Films were formed on quartz slides with a PEI (1 mg mL^{-1} in 500 mM NaCl solution) primer layer.

Bacteria Adsorption Assay. *Escherichia coli* (*E. coli*, American Type Culture Collection (ATCC) #14948) were cultured in Luria broth medium at 37 °C with constant shaking until an optical density at 600 nm (OD600) of 0.6 or ~ 6×10^8 cfu mL^{-1} was obtained. The *E. coli* were then washed in Dulbecco's phosphate-buffered saline (DPBS), and 5×10^7 cfu was added into 8-well chambered glass slides coated with MPN films. The wells were washed with DPBS three times and the bacteria were labeled with LIVE/DEAD BacLight using the supplier's protocol. Finally, adhesion was determined by counting the adhered bacteria in four random spots in each well using an inverted Olympus IX71 microscope with a 60× objective.

Preparation of P(EtOx)-OH and P(EtOx)-Gal. A stock solution containing methyl tosylate (51 mg, 0.25 mmol) and 2-ethyl-2-oxazoline (EtOx, 1.5 g, 15.1 mmol) was prepared in acetonitrile (4.6 g, 112 mmol). The total monomer concentration was adjusted to 2 M to achieve a monomer-to-initiator ratio of 55:1. The stock solution was split equally and introduced in two polymerization vials that were capped under argon. The vials were heated to 85 °C in an oil bath for 7.5 h. After cooling, the polymerization in one vial was terminated by the addition of aqueous

potassium carbonate solution, and the polymer solution was refluxed overnight and worked up by extraction with dichloromethane and precipitation in ice-cold diethyl ether. A 2-fold excess of gallic acid (with respect to the initiator) was added to the other vial and the polymerization mixture was stirred in the dark at room temperature overnight. Subsequently, the polymer solutions were diluted with dichloromethane, washed three times with saturated $NaHCO_3$ and brine, and dried over $MgSO_4$. After concentrating the solutions under reduced pressure, the polymers were precipitated in ice-cold diethyl ether. The conversion and the end group functionalization were calculated to be 91% and 81%, respectively. Size-exclusion chromatography (SEC) (DMAc, LiBr): P(EtOx)-OH M_n = 9040 g mol^{-1}, $Đ$ = 1.22; P(EtOx)-Gal M_n = 10500 g mol^{-1}, $Đ$ = 1.25. ^{1}H-NMR (MeOD, 400 MHz): δ 7.0–6.9 (gallic acid), 3.8–3.3 (N-CH_2), 2.6–2.2 (CH_2 EtOx), 1.2–0.9 (CH_3 EtOx). SEC analyses of the polymer samples were performed in *N*,*N*-dimethylacetamide (DMAc) with 0.03% w/v LiBr and 0.05% 2,6-dibutyl-4-methylphenol using a Shimadzu modular system comprising a DGU-12A degasser, an SIL-10AD automatic injector, a 5.0 μm bead-size guard column (50 mm × 7.8 mm) and an additional four 300 mm × 7.8 mm linear Phenogel columns (bead size: 5.0 μm; pore sizes: 10^5, 10^4, 10^3, and 500 Å), and an RID-10A differential refractive index detector. The temperature of the columns was maintained at 50 °C using a CTO 10A oven, and the flow rate was kept at 1 mL min^{-1} using a LC-10AT pump. A molecular weight calibration curve was produced using commercial narrow molecular weight distribution polystyrene standards with molecular weights ranging from 500 to 10^6 g mol^{-1}. ^{1}H NMR spectra were recorded using a 400 MHz Varian INOVA system at 25 °C.

RESULTS AND DISCUSSION

Layer-by-Layer Assembly and Protein Fouling of TA/Fe^{III} Films. TA/Fe^{III} films were assembled on QCM substrates pre-coated with PEI via LbL assembly by exposing the QCM chips first to TA solution (0.4 mg mL^{-1}), followed by washing with water and subsequent immersion into a solution of $FeCl_3 \cdot 6H_2O$ (0.1 mg mL^{-1}) (**Figure 1a–d**). PEI was used to increase the adhesion and homogeneity of the first layer of TA.[15] After drying the substrates under a gentle stream of N_2, the change in frequency was recorded and the corresponding mass change was calculated. A linear growth of the MPN film was observed (**Figure 2a**) with sequential layer deposition, which is consistent with previous reports that have shown that each bilayer of TA/Fe^{III} is roughly the thickness of a single TA molecule (~2–3 nm).[15] The deposition cycles were repeated at least three times (i.e., $(TA/Fe^{III})_3$) to ensure complete coverage of the substrate,[23,24] followed by exposure to protein solutions. As an example, films capped with either Fe^{III} or TA both showed large mass increases when incubated with FBS (**Figure 2b**), suggesting that the interaction of TA and Fe^{III} with proteins is not inhibited when deposited into films.[10-13] Previous reports have demonstrated that the surface charge of LbL-assembled MPNs is negative (approximately −45 mV) regardless of the capping layer (Fe^{III} or TA), primarily due to the dominant negative charge of TA.[15] Nevertheless, in the context of protein adsorption, the surface charge of the MPN films is not a sufficient descriptor of the surface. As we have previously described using atomic force microscopy force measurements, secondary nonelectrostatic interactions (hydrogen bonding, π–π stacking) also play important roles when MPN surfaces interact with other surfaces or macromolecules.[25]

Previous reports have used proteomics to establish the composition of the adsorbed layer of proteins on surfaces of metal oxide,[26] carbon nanotubes,[27] adsorbed polyelectrolytes,[28] and polymer particles.[29-33] These studies investigated the effect of surface functionality, density,[29,31]

and hydrophobicity,[27,34,35] as well as proteomic profiles. Despite the structural complexity of proteins, a recurrent concept in protein adsorption is that, for protein solutions of purified proteins at the same concentration, the adsorption of proteins with larger molar masses results in higher total adsorbed mass.[27,36] To have a more specific and comparable understanding of protein adsorption on TA/Fe^{III} films, the adsorption of BSA, IgG, and fibrinogen were studied and compared with that of serum, a complex solution of proteins. BSA offers a particularly relevant point of comparison as albumins represent more than half of the protein content in serum. The molar masses (M_N) of the proteins studied are 66 kDa for BSA, 155 kDa for IgG, and 340 kDa for fibrinogen. The degree of hydrophobicity of the proteins increases in the order BSA < IgG < fibrinogen but they bear a similar charge in PBS (i.e., negative at ~pH 7.4).

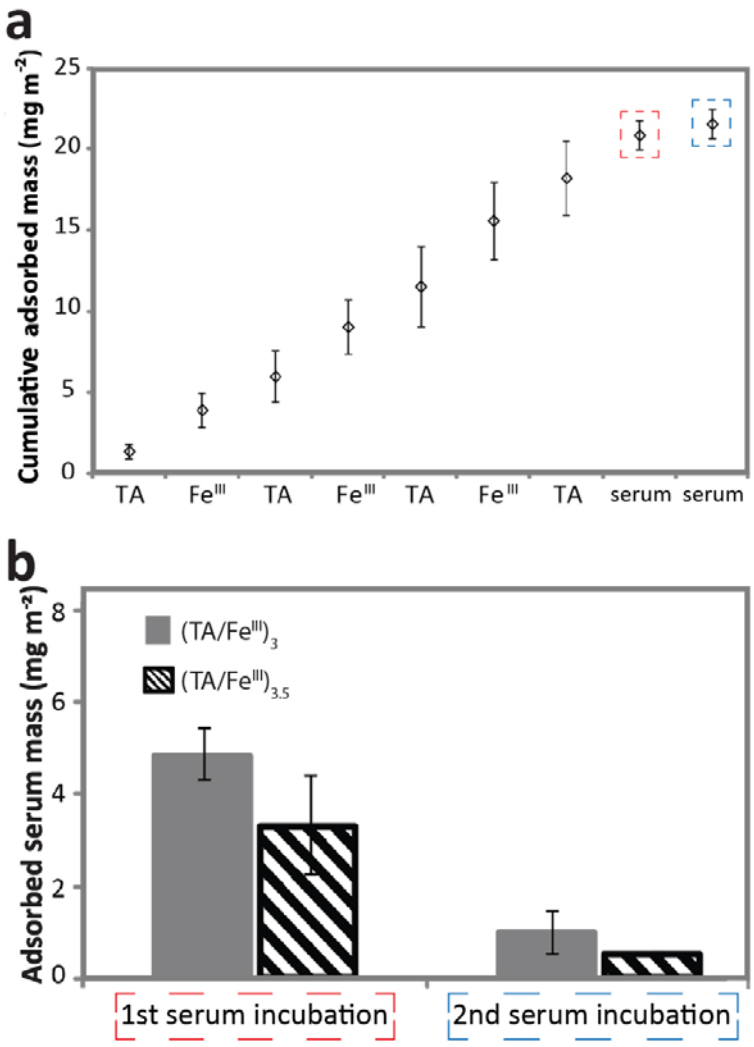

Figure 2. (a) LbL layer growth of a $(TA/Fe^{III})_{3.5}$ film and subsequent serum (FBS) adsorption. (b) Adsorbed mass of serum on (Fe^{III}-terminated) $(TA/Fe^{III})_3$ films and (TA-terminated) $(TA/Fe^{III})_{3.5}$ films measured either after a single exposure to serum or after a second exposure to serum.

For both MPN systems (Fe^{III}-terminated and TA-terminated), larger proteins resulted in larger adsorbed amounts (**Figure 3**), which is consistent with literature findings of studies on the adsorption of the same types of proteins on silicone and plasma-treated polymer surfaces.[37,38] Specifically, the adsorbed mass of both IgG and fibrinogen was more than twice as high as that

of BSA and serum. The fact that the adsorbed mass of BSA matches well with adsorbed serum amounts suggests a potentially dominant adsorption from BSA, which is substantially more abundant in serum. As a final proof, the MPN films were pre-incubated with individual proteins and the protein-coated MPNs were exposed to serum to monitor the different adsorption amounts (**Figure S1**). Very little serum adsorbed onto the IgG- and fibrinogen-coated MPNs compared with the BSA-coated MPNs, further suggesting that higher molecular weight proteins lead to a reduction in serum fouling properties, similarly to what can be seen when examining the adsorption of other macromolecules, such as polymers,[39] possibly due to a larger hydrodynamic thickness from larger macromolecules. This hypothesis is further verified when considering that an adsorption time of 10 min was used, where diffusion-limited behaviors are known to govern adsorption,[40] thereby promoting interactions with smaller proteins that diffuse faster to the surface, adsorb, and prevent the adsorption of larger proteins on the surface. Nevertheless, some intermediate adsorption equilibrium will be reached as this competitive adsorption predominantly occurs over the first minute.[40] Longer exposure times to a mixture of proteins, as is the case in serum, may significantly affect the composition of the adsorbed proteins as has been shown for synthetic polymer systems.[39]

Despite serum proteins adsorbing in substantially larger amounts on Fe^{III}-terminated MPNs, the adsorbed masses for all three individual proteins investigated were larger on TA-terminated MPNs, with smaller adsorption differences when the protein molar mass increases. The importance of the protein M_N on adsorption onto MPNs was reinforced by examining the adsorption of a protein that is considerably smaller than BSA, namely lysozyme (M_N = 14.4 kDa). On TA-terminated MPNs, the adsorbed mass of lysozyme was approximately three times smaller than the adsorbed mass of BSA (1.13 ± 0.8 mg m^{-2} for lysozyme vs 3.15 ± 1.0 mg m^{-2} for

BSA). Lysozyme is positively charged in PBS and is therefore expected to adsorb in smaller amounts if surface charge is the key factor for adsorption. This result suggests that serum proteins other than the ones studied above may adsorb more specifically on the Fe^{III}-terminated MPN surface, as many blood proteins have an affinity for metal ions (e.g., hemoglobin, transferrin). In contrast, as the TA-terminated MPN surface had nearly the same adsorbed mass from serum and solely BSA, it is again suggested that BSA was the predominant protein adsorbing onto TA from serum.

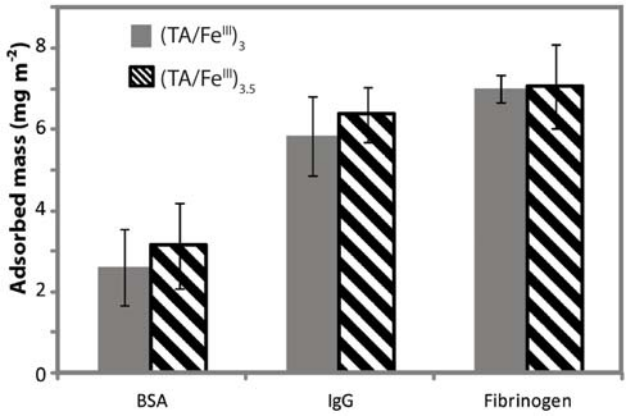

Figure 3. Adsorbed mass of BSA, IgG, and fibrinogen on (Fe^{III}-terminated) $(TA/Fe^{III})_3$ films and (TA-terminated) $(TA/Fe^{III})_{3.5}$ films.

P(EtOx) Functionalization of TA/Fe^{III} Films. Cohesion in MPN films principally arises from the metal ions (i.e., coordination bonds), which suggested that it might be possible to noncovalently modify the films to reduce protein fouling using polymers containing galloyl moieties. Poly(2-ethyl-2-oxazoline) bearing galloyl end groups (P(EtOx)-Gal) was compared against hydroxy-terminated P(EtOx) (P(EtOx)-OH) to determine whether coordinative functionalization was possible. Recently, the interactions of poly(2-isopropyl-2-oxazoline) and poly(2-*n*-propyl-2-oxazoline) with TA were used in LbL assembly; the results have shown that

the two materials can interact noncovalently through hydrogen bonds.[41,42] However, noncovalent chelation-based tethering has not yet been accomplished for MPNs. LbL assembly of MPNs allows for control over the composition of the final layer, thereby ensuring the presence of Fe^{III} for chelation. Poly(2-oxazoline)s are an emerging class of low-fouling polymers with beneficial biomedical properties and a highly functional polymer platform.[43-47] The relative ease of polymerizing the monomers and potential to generate tailor-made low-fouling/stealth polymers make them highly interesting polymeric building blocks with tunable properties for numerous applications.[48,49] The P(EtOx) polymers were prepared by cationic ring-opening polymerization of 2-ethyl-2-oxazoline. For subsequent functionalization with hydroxy and galloyl end groups, the living polymer chains were terminated by treatment with aqueous potassium carbonate solution and gallic acid, respectively.

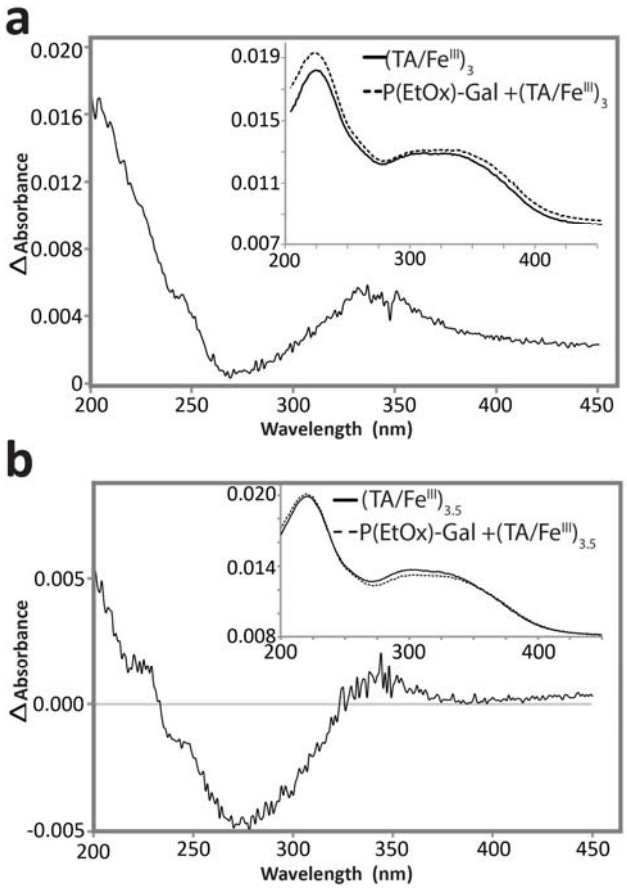

Figure 4. UV-Vis absorption spectra obtained by subtracting the MPN spectrum from the P(EtOx)-Gal-functionalized (a) $(TA/Fe^{III})_3$ MPN film and (b) $(TA/Fe^{III})_{3.5}$ MPN film spectra. Insets show the original spectra used in the subtraction (solid line, before P(EtOx)-Gal functionalization; dashed line, after P(EtOx)-Gal functionalization).

The interaction of P(EtOx)-Gal with MPNs was first investigated with different end layers (TA vs Fe^{III}) to determine if the low-fouling P(EtOx) could be tethered to MPNs through chelation. UV-Vis analysis demonstrated an increase in absorbance at ~210 nm and ~335 nm for the P(EtOx)-Gal-functionalized (Fe^{III}-terminated) $(TA/Fe^{III})_3$ films (**Figure 4a**). The spectrum in Figure 4a was obtained by subtraction of the absorbance spectrum of the bare $(TA/Fe^{III})_3$ (inset in Figure 4a) from that of the P(EtOx)-Gal-functionalized $(TA/Fe^{III})_3$ (inset in Figure 4a). Therefore, the increase in absorbance at 210 nm was likely from the galloyl group, whereas the increase in absorbance at higher wavelengths, 335 nm, was due to coordination between the galloyl group on P(EtOx)-Gal and Fe^{III} in the film.[15] A control experiment not using chelation as the driving force i.e. by monitoring P(EtOx)-Gal adsorption on a (TA-terminated) $(TA/Fe^{III})_{3.5}$ film displayed a similar peak at ~210 nm, highlighting the presence of the Gal end functionality of the polymer, but no substantial increase in absorbance at 335 nm, which suggested a lack of chelation (**Figure 4b**). The negative changes in absorbance values observed between 230 and 320 nm in **Figure 4b** may correspond to desorption of TA from the MPN film owing to competitive adsorption process involving Fe^{III} and P(EtOx)-Gal, as seen in previous studies.[50] In addition, XPS measurements showed a significant increase in the nitrogen content from the N1s region of the spectrum after P(EtOx)-Gal functionalization (**Figure S2** and **Figure S3**), further suggesting the presence of the nitrogen-containing P(EtOx) polymer. To further elucidate the

mechanism of functionalization and the fouling properties of the modified films, comparison experiments with P(EtOx)-OH, which does not contain the chelation site, were conducted.

Both P(EtOx)-OH and P(EtOx)-Gal adsorbed onto the Fe^{III}-terminated MPN films in similar amounts as confirmed by QCM, (**Figure 5a**). The (TA-terminated) $(TA/Fe^{III})_{3.5}$ films functionalized with either P(EtOx)-OH or P(EtOx)-Gal displayed comparable R_{RMS} values (~1.5 nm) as measured by AFM (**Figure S4** and **Table S1**), suggesting a similar deposition mechanism through hydrogen bonding between TA and P(EtOx) regardless of the end group. Moreover, the R_{RMS} values were similar to that of the nonfunctionalized (TA-terminated) $(TA/Fe^{III})_{3.5}$ film (1.2 nm). Likewise, functionalization with P(EtOx)-OH did not yield a significant change in roughness (0.7 nm for the nonfunctionalized film vs 0.5 nm for the functionalized film) for the (Fe-terminated) $(TA/Fe^{III})_3$ films; however, functionalization with P(EtOx)-Gal led to nearly a doubling of the R_{RMS} from ~0.7 nm (nonfunctionalized film) to ~1.3 nm (functionalized film) (**Table S1**). This again suggested that the P(EtOx)-Gal was tethered through chelation and could then partially orient away from the films in a globular fashion, thereby increasing the roughness. Advancing contact angle measurements yielded similar results to the R_{RMS} measurements where functionalization with P(EtOx)-Gal resulted in lower contact angles than functionalization of (Fe^{III}-terminated) $(TA/Fe^{III})_3$ films with P(EtOx)-OH, implying that the orientation of the hydrophilic P(EtOx) polymer is away from the MPN surface (**Table S1**). Differences in R_{RMS} are coupled with corresponding changes in the static contact angle, whereby an increase in surface roughness enhances the underlying hydrophilicity of the surface,[51] and correlation between R_{RMS} and contact angle was evident for the different modified MPN films (**Figure S5**).

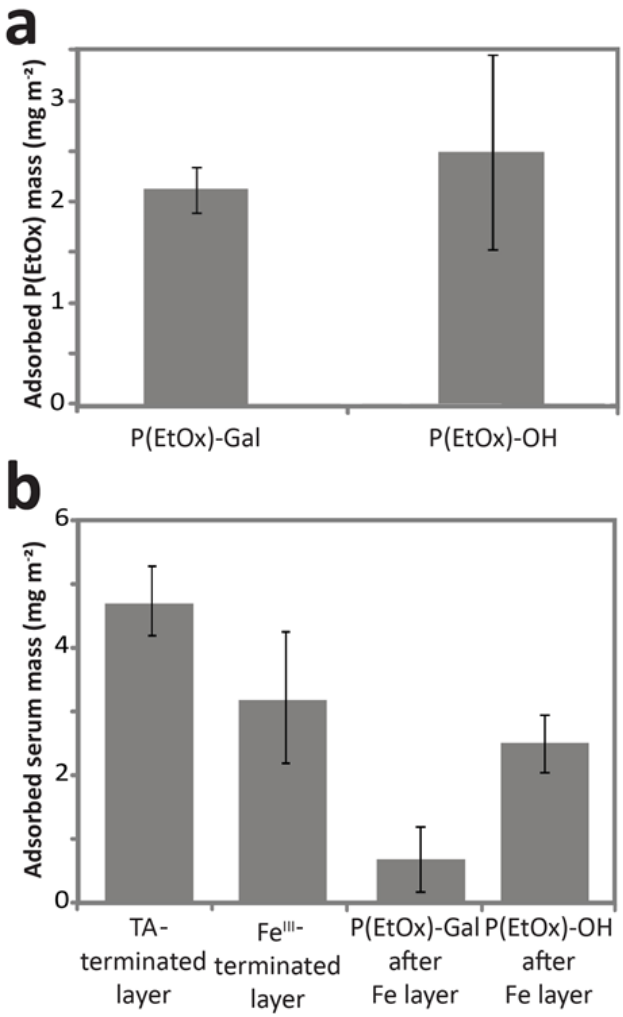

Figure 5. (a) P(EtOx)-Gal and P(EtOx)-OH adsorption on (Fe^{III}-terminated) $(TA/Fe^{III})_3$ film as measured by QCM in the dry state. (b) Adsorbed mass of serum on $(TA/Fe^{III})_3$ or $(TA/Fe^{III})_{3.5}$ films with an Fe^{III}- or TA-terminated layer, respectively, or $(TA/Fe^{III})_3$ films functionalized with PEtOx bearing different terminal groups (Gal or OH).

Protein and Bacterial Fouling of P(EtOx)-Functionalized TA/Fe^{III} Films. Compared with the R_{RMS} of the P(EtOx)-OH-functionalized (Fe^{III}-terminated) $(TA/Fe^{III})_3$ film, the higher R_{RMS} of the P(EtOx)-Gal-functionalized (Fe^{III}-terminated) $(TA/Fe^{III})_3$ film is expected to lead to a larger amount of adsorbed protein owing to the higher surface area assuming that both P(EtOx) films are truly similar in surface chemistry. However, the P(EtOx)-Gal-functionalized (Fe^{III}-

terminated) $(TA/Fe^{III})_3$ had a much lower protein fouling than the P(EtOx)-OH-functionalized (Fe^{III}-terminated) $(TA/Fe^{III})_3$ film (**Figure 5b**), which again supports the concept that P(EtOx)-Gal was interacting specifically with the Fe layer of the MPN films. In contrast, P(EtOx)-OH interacted with the films through hydrogen bonding across the whole polymer, rather than at the end site only, as shown previously in polymer/TA LbL assembly studies.[52,53] Specifically, functionalization with P(EtOx)-OH reduced the adsorption of serum proteins by ~49% but functionalization with P(EtOx)-Gal showed a better reduction in serum adsorption (~86%) (**Figure 5b**) relative to the mass adsorption observed for the corresponding nonfunctionalized film. A previous report comparing low-fouling PEG-catechol/Fe^{III} capsules with TA/Fe^{III} capsules demonstrated that PEG-based MPN capsules displayed ~80% lower fouling than TA-based MPN capsules.[8] Although our MPN films were functionalized with P(EtOx) rather than being solely composed of low-fouling materials, the similar fouling values obtained to those of systems composed principally of PEG highlight that the present MPN films are uniformly coated with P(EtOx)-Gal. Overall, these observations highlight that even though protein adsorption is reduced from simple, nonspecific PEtOx adsorption, the specific conjugation of galloyl-terminated polymers to Fe^{III} is necessary to engineer surfaces with significantly reduced surface–protein interactions.

To quantitatively correlate the differences between the pristine and P(EtOx)-Gal-functionalized (Fe^{III}-terminated) $(TA/Fe^{III})_3$ film, protein adsorption experiments were performed with solutions of BSA, IgG, and fibrinogen. The adsorption of all three proteins was reduced after P(EtOx)-Gal functionalization when compared to adsorption on the pristine (Fe^{III}-terminated) $(TA/Fe^{III})_3$ MPN film (**Figure 6**). The reduction in adsorbed protein mass of ~2.5 mg m^2 was similar for all three proteins when comparing the pristine and P(EtOx)-Gal-

functionalized MPN films. However, in relative terms ~90% less BSA adsorbed onto the P(EtOx)-OH-functionalized (Fe^{III}-terminated) $(TA/Fe^{III})_3$ film. Nonspecific binding constants of IgG and fibrinogen are assumed to be considerably higher than that of serum albumin.[37,38,40] Thus, it is likely that the PEtOx-Gal coating simply raised these binding constants.

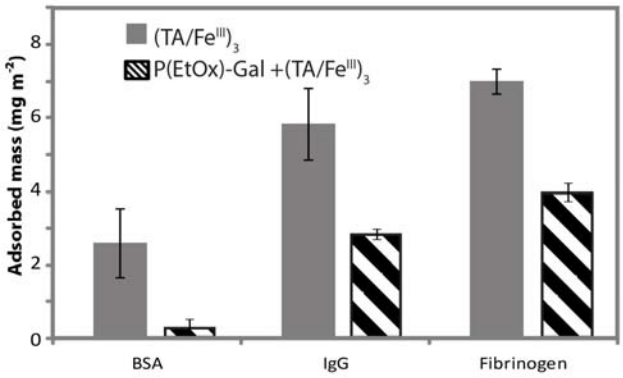

Figure 6. Adsorbed mass of BSA, IgG, and fibrinogen on P(EtOx)-Gal-functionalized $(TA/Fe^{III})_3$ films and nonfunctionalized $(TA/Fe^{III})_3$ films.

To determine whether the reduced protein fouling could be generalized to a more complex system, bacterial adsorption tests were performed. First, it was determined that the films did not have any effect on bacterial viability as the OD600 of the bacterial suspension continued to increase even after longer (>4 h) exposure to the MPN films. Fe^{III}-terminated MPN films and the corresponding P(EtOx)-functionalized films were examined. Both P(EtOx)-functionalized films showed ~66% reduced bacterial adhesion (**Figure 7** and **Figure S6**). However, with larger biological systems (i.e., bacteria) involved, the presence of P(EtOx) alone was enough to reduce fouling regardless of orientation as both functionalization with P(EtOx)-Gal and P(EtOx)-OH showed reduced adsorption **(Figure 7**). Nevertheless, this reduction in bacteria adsorption is not as efficient when compared with some other polyphenol coatings functionalized by *grafting-from*

strategies, or for other surfaces aimed specifically at antifouling characteristics, where polymeric *grafting-from* is a preferred strategy to *grafting-to*.[22]

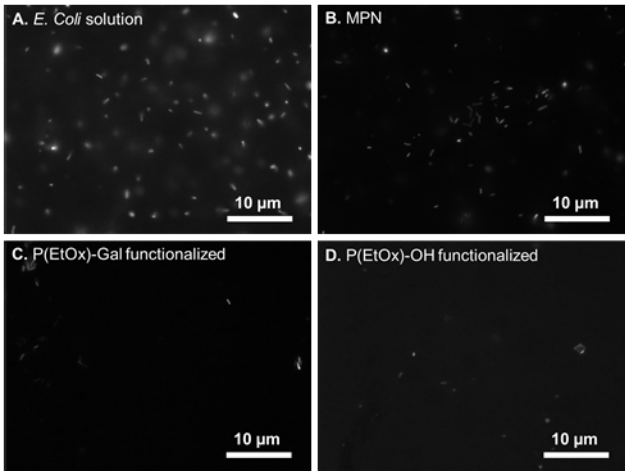

Figure 7. Representative fluorescence microscopy images of bacteria (*E. coli*) (a) in solution and adsorbed onto (b) pristine (Fe^{III}-terminated) $(TA/Fe^{III})_3$, (c) P(EtOx)-Gal-functionalized (Fe^{III}-terminated) $(TA/Fe^{III})_3$, and (d) P(EtOx)-OH-functionalized (Fe^{III}-terminated) $(TA/Fe^{III})_3$ MPN films.

CONCLUSIONS

We have reported the formation of layer-by-layer TA/Fe^{III} MPN films and have quantified protein and serum adsorption onto the films as a function of the composition of the terminal layer and charge of the protein. Higher molecular weight proteins adsorbed in higher amounts on MPNs. Additionally, we have demonstrated the possibility of using partially coordinated Fe^{III} ions as a means of adding specific functionality through the chelation of galloyl-terminated P(EtOx), which reduced protein adsorption by 86% and bacterial adhesion by ~66%. In absolute terms, the reduction of protein adsorption was similar for all three proteins studied. However, in relative terms, the adsorption of smaller proteins was greatly reduced. We anticipate that other

galloyl-terminated polymers could also be used for surface functionalization, potentially opening up routes for adding targeting moieties, therapeutics, or imaging agents to MPN films and capsules.

ASSOCIATED CONTENT

Supporting information. Protein adsorption mass post serum adsorption, AFM images used for R_{RMS} analysis, XPS spectra, contact angle–R_{RMS} correlation.

AUTHOR INFORMATION

Corresponding Author

*E-mail: fcaruso@unimelb.edu.au.

Present Addresses

†Department of Bioproducts and Biosystems, School of Chemical Engineering, Aalto University, FI-00076 Aalto, Finland

‡ARC Centre of Excellence in Convergent Bio-Nano Science and Technology, and Monash Institute of Pharmaceutical Sciences, Monash University, Parkville, Victoria 3052, Australia

§Department of Materials Engineering, The University of Tokyo, 7-3-1 Hongo, Bunkyoku, Tokyo 113-8656, Japan

Author Contributions

The manuscript was written through contributions of all authors. All authors have given approval to the final version of the manuscript.

Funding Sources

This research was conducted and funded by the Australian Research Council (ARC) Centre of Excellence in Convergent Bio-Nano Science and Technology (project no. CE140100036) and an ARC Discovery Project (DP170103331). F.C. acknowledges the award of a National Health and Medical Research Council Senior Principal Research Fellowship (APP1135806). This work was performed in part at the Materials Characterisation and Fabrication Platform at The University of Melbourne and the Victorian Node of the Australian National Fabrication Facility.

ACKNOWLEDGMENT

K. Kempe acknowledges the Alexander von Humboldt Foundation for a Feodor Lynen Research Fellowship.

REFERENCES

1. Richardson, J. J.; Björnmalm, M.; Caruso, F. Technology-Driven Layer-By-Layer Assembly of Nanofilms. *Science* **2015**, *348*, aaa2491.
2. Sileika, T. S.; Barrett, D. G.; Zhang, R.; Lau, K. H. A.; Messersmith, P. B. Colorless Multifunctional Coatings Inspired by Polyphenols Found in Tea, Chocolate, and Wine. *Angew. Chem. Int. Ed.* **2013**, *41*, 10966-10970.
3. Lee, H.; Dellatore, S. M.; Miller, W. M.; Messersmith, P. B. Mussel-Inspired Surface Chemistry for Multifunctional Coatings. *Science* **2007**, *318*, 426-430.
4. Barrett, D. G.; Sileika, T. S.; Messersmith, P. B., Molecular Diversity in Phenolic and Polyphenolic Precursors of Tannin-Inspired Nanocoatings. *Chem. Commun.* **2014**, *50*, 7265-7268.
5. Ejima, H.; Richardson, J. J.; Liang, K.; Best, J. P.; van Koeverden, M. P.; Such, G. K.; Cui, J.; Caruso, F. One-Step Assembly of Coordination Complexes for Versatile Film and Particle Engineering. *Science* **2013**, *341*, 154-157.
6. Guo, J.; Ping, Y.; Ejima, H.; Alt, K.; Meissner, M.; Richardson, J. J.; Yan, Y.; Peter, K.; von Elverfeldt, D.; Hagemeyer, C. E. Engineering Multifunctional Capsules through the Assembly of Metal–Phenolic Networks. *Angew. Chem. Int. Ed.* **2014**, *53*, 5546-5551.
7. Tardy, B. L.; Richardson, J. J.; Guo, J.; Lehtonen, J.; Ago, M.; Rojas, O. J. Lignin Nano- and Microparticles as Template for Nanostructured Materials: Formation of Hollow Metal-Phenolic Capsules. *Green Chem.* **2018**, *20*, 1335-1344.
8. Ju, Y.; Cui, J.; Müllner, M.; Suma, T.; Hu, M.; Caruso, F. Engineering Low-Fouling and pH-Degradable Capsules through the Assembly of Metal-Phenolic Networks. *Biomacromolecules* **2015**, *16*, 807-814.

9. Ju, Y.; Cui, J.; Sun, H.; Müllner, M.; Dai, Y.; Guo, J.; Bertleff-Zieschang, N.; Suma, T.; Richardson, J. J.; Caruso, F. Engineered Metal-Phenolic Capsules Show Tunable Targeted Delivery to Cancer Cells. *Biomacromolecules* **2016**, *17*, 2268-2276.
10. Hagerman, A. E.; Butler, L. G. Protein Precipitation Method for the Quantitative Determination of Tannins. *J. Agric. Food Chem.* **1978**, *26*, 809-812.
11. Boyden, S. V. The Adsorption of Proteins on Erythrocytes Treated with Tannic Acid and Subsequent Hemagglutination by Antiprotein Sera. *J. Exp. Med.* **1951**, *93*, 107-120.
12. Horie, M.; Nishio, K.; Fujita, K.; Endoh, S.; Miyauchi, A.; Saito, Y.; Iwahashi, H.; Yamamoto, K.; Murayama, H.; Nakano, H. Protein Adsorption of Ultrafine Metal Oxide and Its Influence on Cytotoxicity toward Cultured Cells. *Chem. Res. Toxicol.* **2009**, *22*, 543-553.
13. Ruh, H.; Kühl, B.; Brenner-Weiss, G.; Hopf, C.; Diabaté, S.; Weiss, C. Identification of Serum Proteins Bound to Industrial Nanomaterials. *Toxicol. Lett.* **2012**, *208*, 41-50.
14. McGuire, C. V.; Forgan, R. S. The Surface Chemistry of Metal–Organic Frameworks. *Chem. Commun.* **2015**, *51*, 5199-5217.
15. Rahim, M. A.; Ejima, H.; Cho, K. L.; Kempe, K.; Müllner, M.; Best, J. P.; Caruso, F. Coordination-Driven Multistep Assembly of Metal–Polyphenol Films and Capsules. *Chem. Mater.* **2014**, *26*, 1645-1653.
16. Kim, S.; Kim, D. S.; Kang, S. M. Reversible Layer-by-Layer Deposition on Solid Substrates Inspired by Mussel Byssus Cuticle. *Chem.– Asian J.* **2014**, *9*, 63-66.
17. Richardson, J. J.; Cui, J.; Björnmalm, M.; Braunger, J. A.; Ejima, H.; Caruso, F. Innovation in Layer-by-Layer Assembly. *Chem. Rev.* **2016**, *116*, 14828-14867.
18. Ren, P. F.; Yang, H. C.; Liang, H. Q.; Xu, X. L.; Wan, L. S.; Xu, Z. K., Highly Stable, Protein-Resistant Surfaces via the Layer-by-Layer Assembly of Poly(sulfobetaine methacrylate) and Tannic Acid. *Langmuir* **2015**, *31*, 5851-5858.
19. Kim, S.; Gim, T.; Kang, S. M. Versatile, Tannic Acid-Mediated Surface PEGylation for Marine Antifouling Applications. *ACS Appl. Mater. Interfaces* **2015**, *7*, 6412-6416.
20. Han, L.; Liu, Q.; Yang, L.; Ye, T.; He, Z.; Jia, L. Facile Oriented Immobilization of Histidine-Tagged Proteins on Nonfouling Cobalt Polyphenolic Self-Assembly Surfaces. *ACS Biomater. Sci. Eng.* **2017**, *3*, 3328-3337.
21. Xu, L. Q.; Pranantyo, D.; Neoh, K. G.; Kang, E. T.; Fu, G. D. Thiol Reactive Maleimido-Containing Tannic Acid for the Bioinspired Surface Anchoring and Post-Functionalization of Antifouling Coatings. *ACS Sustainable Chem. Eng.* **2016**, *4*, 4264-4272.
22. Pranantyo, D.; Xu, L. Q.; Neoh, K. G.; Kang, E. T.; Ng, Y. X.; Teo, S. L. M. Tea Stains-Inspired Initiator Primer for Surface Grafting of Antifouling and Antimicrobial Polymer Brush Coatings. *Biomacromolecules* **2015**, *16*, 723-732.
23. Ladam, G.; Schaad, P.; Voegel, J.; Schaaf, P.; Decher, G.; Cuisinier, F. In Situ Determination of the Structural Properties of Initially Deposited Polyelectrolyte Multilayers. *Langmuir* **2000**, *16*, 1249-1255.
24. Caruso, F.; Niikura, K.; Furlong, D. N.; Okahata, Y., 1. Ultrathin Multilayer Polyelectrolyte Films On Gold: Construction and Thickness Determination. *Langmuir* **1997**, *13*, 3422-3426.
25. Guo, J.; Tardy, B. L.; Christofferson, A. J.; Dai, Y.; Richardson, J. J.; Zhu, W.; Hu, M.; Ju, Y.; Cui, J.; Dagastine, R. R., Modular Assembly of Superstructures from Polyphenol-Functionalized Building Blocks. *Nat. Nanotechnol.* **2016**, *11*, 1105.

26. Casals, E.; Pfaller, T.; Duschl, A.; Oostingh, G. J.; Puntes, V. F., Hardening of the Nanoparticle–Protein Corona in Metal (Au, Ag) and Oxide (Fe_3O_4, CoO, and CeO_2) Nanoparticles. *Small* **2011**, *7*, 3479-3486.
27. Shannahan, J. H.; Brown, J. M.; Chen, R.; Ke, P. C.; Lai, X.; Mitra, S.; Witzmann, F. A. Comparison of Nanotube–Protein Corona Composition in Cell Culture Media. *Small* **2013**, *9*, 2171–2181.
28. Wiogo, H. T.; Lim, M.; Bulmus, V.; Gutiérrez, L. a.; Woodward, R. C.; Amal, R. Insight into Serum Protein Interactions with Functionalized Magnetic Nanoparticles in Biological Media. *Langmuir* **2012**, *28*, 4346-4356.
29. Ehrenberg, M. S.; Friedman, A. E.; Finkelstein, J. N.; Oberdörster, G.; McGrath, J. L., The Influence of Protein Adsorption on Nanoparticle Association with Cultured Endothelial Cells. *Biomaterials* **2009**, *30*, 603-610.
30. Cedervall, T.; Lynch, I.; Foy, M.; Berggård, T.; Donnelly, S. C.; Cagney, G.; Linse, S.; Dawson, K. A. Detailed Identification of Plasma Proteins Adsorbed on Copolymer Nanoparticles. *Angew. Chem. Int. Ed.* **2007**, *46*, 5754-5756.
31. Lundqvist, M.; Stigler, J.; Elia, G.; Lynch, I.; Cedervall, T.; Dawson, K. A. Nanoparticle Size and Surface Properties Determine the Protein Corona with Possible Implications for Biological Impacts. *Proc. Natl. Acad. Sci. U.S.A.* **2008**, *105*, 14265-14270.
32. Cho, W.-S.; Thielbeer, F.; Duffin, R.; Johansson, E. M.; Megson, I. L.; MacNee, W.; Bradley, M.; Donaldson, K. Surface Functionalization Affects the Zeta Potential, Coronal Stability and Membranolytic Activity of Polymeric Nanoparticles. *Nanotoxicology* **2014**, *8*, 202–211.
33. Ju, Y.; Dai, Q.; Cui, J.; Dai, Y.; Suma, T.; Richardson, J. J.; Caruso, F. Improving Targeting of Metal–Phenolic Capsules by the Presence of Protein Coronas. *ACS Appl. Mater. Interfaces* **2016**, *8*, 22914-22922.
34. Roach, P.; Farrar, D.; Perry, C. C. Surface Tailoring for Controlled Protein Adsorption: Effect of Topography at the Nanometer Scale and Chemistry. *J. Am. Chem. Soc.* **2006**, *128*, 3939-3945.
35. Prime, K. L.; Whitesides, G. M. Self-Assembled Organic Monolayers: Model Systems for Studying Adsorption of Proteins at Surfaces. *Science* **1991**, *252*, 1164-1167.
36. Treuel, L.; Nienhaus, G. U. Toward a Molecular Understanding of Nanoparticle–Protein Interactions. *Biophys. Rev.* **2012**, *4*, 137-147.
37. Warkentin, P.; Wälivaara, B.; Lundström, I.; Tengvall, P. Differential Surface Binding of Albumin, Immunoglobulin G and Fibrinogen. *Biomaterials* **1994**, *15*, 786-795.
38. Malmsten, M.; Muller, D.; Lassen, B., Sequential Adsorption of Human Serum Albumin (HSA), Immunoglobulin G (IgG), and Fibrinogen (Fgn) at HMDSO Plasma Polymer Surfaces. *J. Colloid Interface. Sci.* **1997**, *193*, 88-95.
39. Mubarekyan, E.; Santore, M. M. Influence of Molecular Weight and Layer Age on Self-Exchange Kinetics for Saturated Layers of PEO in a Good Solvent. *Macromolecules* **2001**, *34*, 4978-4986.
40. Vilaseca, P.; Dawson, K. A.; Franzese, G. Understanding and Modulating the Competitive Surface-Adsorption of Proteins through Coarse-Grained Molecular Dynamics Simulations. *Soft Matter* **2013**, *9*, 6978–6985.
41. Erel, I.; Schlaad, H.; Demirel, A. L. Effect of Structural Isomerism and Polymer End Group on the pH-Stability of Hydrogen-Bonded Multilayers. *J. Colloid Interface Sci.* **2011**, *361*, 477-482.

42. da Fonseca Antunes, A. B.; Dierendonck, M.; Vancoillie, G.; Remon, J. P.; Hoogenboom, R.; De Geest, B. G. Hydrogen Bonded Polymeric Multilayer Films Assembled Below and Above the Cloud Point Temperature. *Chem. Commun.* **2013**, *49*, 9663-9665.
43. Kempe, K.; Hoogenboom, R.; Jaeger, M.; Schubert, U. S. Three-Fold Metal-Free Efficient ("Click") Reactions onto a Multifunctional Poly(2-oxazoline) Designer Scaffold. *Macromolecules* **2011**, *44*, 6424-6432.
44. Guillerm, B.; Monge, S.; Lapinte, V.; Robin, J. J. How to Modulate the Chemical Structure of Polyoxazolines by Appropriate Functionalization. *Macromol. Rapid Commun.* **2012**, *33*, 1600-1612.
45. Kempe, K. Chain and Step Growth Polymerizations of Cyclic Imino Ethers: From Poly(2-oxazoline)s to Poly(ester amide)s. *Macromol. Chem. Phys.* **2017**, *218*, 1700021.
46. Luxenhofer, R.; Han, Y.; Schulz, A.; Tong, J.; He, Z.; Kabanov, A. V.; Jordan, R. Poly(2-oxazoline)s as Polymer Therapeutics. *Macromol. Rapid Commun.* **2012**, *33*, 1613-1631.
47. Sedlacek, O.; Monnery, B. D.; Filippov, S. K.; Hoogenboom, R.; Hruby, M. Poly(2-Oxazoline)s–Are They More Advantageous for Biomedical Applications Than Other Polymers? *Macromol. Rapid Commun.* **2012**, *33*, 1648-1662.
48. Konradi, R.; Acikgoz, C.; Textor, M. Polyoxazolines for Nonfouling Surface Coatings—A Direct Comparison to the Gold Standard PEG. *Macromol. Rapid Commun.* **2012**, *33*, 1663-1676.
49. Tauhardt, L.; Kempe, K.; Gottschaldt, M.; Schubert, U. S. Poly(2-oxazoline) Functionalized Surfaces: From Modification to Application. *Chem. Soc. Rev.* **2013**, *42*, 7998-8011.
50. Yang, L.; Han, L.; Ren, J.; Wei, H.; Jia, L. Coating Process and Stability of Metal-Polyphenol Film. *Colloid Surf., A* **2015**, *484*, 197-205.
51. De Gennes, P.-G.; Brochard-Wyart, F.; Quéré, D. *Capillarity and Wetting Phenomena: Drops, Bubbles, Pearls, Waves*. Springer: 2004.
52. Haktaniyan, M.; Atilla, S.; Cagli, E.; Erel-Goktepe, I. pH-and Temperature-Induced Release of Doxorubicin from Multilayers of Poly(2-isopropyl-2-oxazoline) and Tannic Acid. *Polym. Int.* **2017**, *66*, 1851-1863.
53. Sundaramurthy, A.; Vergaelen, M.; Maji, S.; Auzély-Velty, R.; Zhang, Z.; De Geest, B. G.; Hoogenboom, R. Hydrogen Bonded Multilayer Films Based on Poly(2-oxazoline)s and Tannic Acid. *Adv. Healthcare Mater.* **2014**, *3*, 2040-2047.

Table of Contents Use Only

Protein Adsorption and Coordination-Based End-Tethering of Functional Polymers on Metal–Phenolic Network Films

Blaise L. Tardy, Joseph J. Richardson, Vichida Nithipipat, Kristian Kempe, Junling Guo, Kwun Lun Cho, Md. Arifur Rahim, Hirotaka Ejima, and Frank Caruso

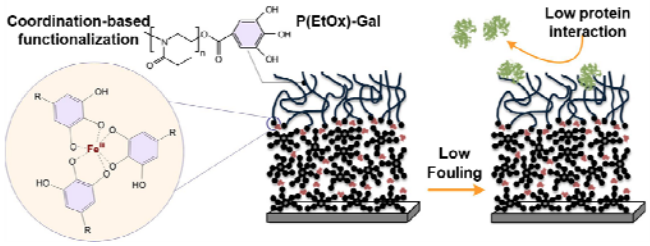

Author/s:
Tardy, BL; Richardson, JJ; Nithipipat, V; Kempe, K; Guo, J; Cho, KL; Rahim, MA; Ejima, H; Caruso, F

Title:
Protein Adsorption and Coordination-Based End-Tethering of Functional Polymers on Metal-Phenolic Network Films

Date:
2019-03-01

Citation:
Tardy, B. L., Richardson, J. J., Nithipipat, V., Kempe, K., Guo, J., Cho, K. L., Rahim, M. A., Ejima, H. & Caruso, F. (2019). Protein Adsorption and Coordination-Based End-Tethering of Functional Polymers on Metal-Phenolic Network Films. BIOMACROMOLECULES, 20 (3), pp.1421-1428. https://doi.org/10.1021/acs.biomac.9b00006.